J. Electrochem. Sci. Eng. **14(5)** (2024) 601-615; http://dx.doi.org/10.5599/jese.2368

Open Access : : ISSN 1847-9286
https://pub.iapchem.org/ojs/index.php/JESE

Original scientific paper

Highly stable and selective determination of glucose by a modified glassy carbon electrode based on micro-rods [Ni(HL)NCS] complex as a novel modifier

Mohammad Javad Khatami, Mohammad Mazloum-Ardakani✉, Hamideh Mohammadian-Sarcheshmeh and Rasoul Vafazadeh

Department of Chemistry, Faculty of Science, Yazd University, Yazd, Iran

Corresponding authors: ✉ *mazloum@yazd.ac.ir ; Tel.: 00983518211670; Fax: 00983518210644*

Received: May 14, 2024; Accepted: August 20, 2024; Published: August 29, 2024

Abstract

Non-enzymatic glucose sensors have acquired a lot of attention, where the modifier materials perform as an electrocatalyst instead of an enzyme on the surface of electrodes. More active sites increased synergistic reactions, and expanded contacts between the electrolyte and the catalyst are essential to enhance catalytic performances. Numerous efforts have been made to fabricate novel non-enzymatic glucose sensors with electrode modification strategies. Herein, a non-enzymatic electrochemical glucose sensor was constructed by a modified glassy carbon electrode based on micro-rods nickel complex as a novel modifier for glucose detection. In alkali media, the non-enzymatic glucose sensor showed a linear dynamic range of 100-1100 µM with an excellent limit of detection of 15.8 µM (S/N = 3). The proposed sensor demonstrated remarkable stability (after recording 50 continuous CV cycles), good reproducibility, and significant anti-interference performance toward fructose, ascorbic acid, dopamine, citric acid, uric acid and sucrose. According to this study, complexes can be an excellent suggestion to fabricate non-enzymatic glucose sensors.

Keywords

Glucose; non-enzymatic sensor; Ni complex, stability; selectivity; human blood serum

Introduction

Glucose is a vital component for sustaining life, as it serves as a direct energy source in metabolic processes, enabling the maintenance of usual life activities. Glucose is widely present in the blood-stream of living organisms [1]. Glucose detection, including non-enzymatic and enzymatic detection, is important to meet the growing needs for clinical diagnosis and ecological and food monitoring [2,3]. In the field of clinical medicine, one of the most effective causes of death and disability in the world is diabetes. As stated by the World Health Organization (WHO), there are 450 million cases of diabetes

worldwide, and this number may increase to 700 million by 2045. Nowadays, the blood glucose concentration is the principal basis for diagnosing diabetes. The standard was defined by the WHO in 2009: the fasting blood glucose (FBG) of normal people is 3.9 to 6.1 mM, and the blood glucose 2 h after a meal is 7.8 mM or less [4]. If the blood glucose level is different from the normal range, it will hurt the blood vessels, heart, nerves, kidneys, and eyes, as well as diseases of the circulatory system. Long-term complications of hyperglycemia can be divided into macrovascular complications of diabetes (such as heart disease) and microvascular complications of diabetes that lead to organ damage (such as nephropathy, retinopathy, and neuropathy) [5]. Diabetes Mellitus is one of the significant problems threatening human health, and there has always been a demand for quick, economical, and accurate diagnosis of such diseases. Various techniques are used to detect glucose, such as electrochemical methods, optical methods, and spectroscopy. Electrochemical methods have attracted attention owing to their cost-effective, rapid, selective, wide linear range, uncomplicated operation, and reliable processes [6]. Electrochemical sensors have made significant progress in recent years. Extensive research has been reported using them [7-11].

The first generation of glucose sensors are enzyme sensors that have been used in medical diagnosis due to the selectivity and sensitivity of the enzymes. However, they are confined by some environmental parameters, *e.g.,* pH and temperature. Also, they are usually unstable, and their production is expensive [12-15]. Non-enzymatic glucose sensors are considered to cover the limitations of enzymatic sensors. They usually operate based on the response from glucose oxidation [16-18]. Glucose detection by a non-enzymatic sensor has acquired a lot of attention due to its good sensitivity, simplicity, low cost, and adaptability to miniaturization, which omit the limitations of enzymatic sensors. Various materials, such as nanomaterials, complexes, and polymeric materials, can develop non-enzymatic sensors. Metals such as nickel, gold, platinum, metal alloys such as PtPb, PtPd, PdCu, and metal oxides such as Co_3O_4, RuO_2, NiO are used for the fabricating of non-enzymatic sensors because of their excellent catalytic performance. Among these metals, nickel is the best choice as a cheap, sensitive, and selective non-enzymatic electrode material. Also, nickel and nickel hydroxide have good catalytic performance in alkaline environments [19]. These materials can be used to modify electrodes. They are physically fixed on the electrode surface and catalyse glucose oxidation, improving responses and limit of detection (LOD) value [20]. Revenga-Parra *et al.* utilized a Ni complex on the modified screen-printed electrodes with CNT for glucose oxidation and reported LOD = 12 μM [21]. A modified electrode was reported using a nickel complex with graphite/boron-doped diamond (Ni-MG-BDD). It was prepared by thermal etching BDD with Ni. It showed an acceptable electrocatalytic performance and increased conductivity. Finally, good results were obtained with linear dynamic range (LDR) = 0.002 to 0.5 and 0.5 to 15.5 mM and the LOD = 0.24 μM [22]. In electrochemistry, Schiff base complexes featuring various metals have found recent applications. These complexes utilize the central atom (Ni) as a catalyst, owing to its surface oxidation properties and its ability to catalyse reactions involving alcoholic functional groups [23]. Schiff bases are a group of compounds formed by condensation of primary amine with aldehyde or ketones under specific conditions. They can be prepared easily and they have the ability to form complexes with transition metal ions such as Ni(II), Zn(II), Cu(II), *etc*. The catalytic activity of the Ni-Schiff base can be attributed to the presence of $Ni(OH)_2$ and NiOOH species. It is suggested that the oxidation of glucose on the modified electrode takes place through a reaction with Ni(III) species that are generated on the electrode surface. In this process, Ni(III) acts as an electron transfer mediator, facilitating the oxidation of organic compounds like glucose and alcohols [24].

In this work, a non-enzymatic electrochemical glucose sensor based on a glassy carbon electrode (GCE) modified by micro-rods nickel complex (MR-NiC/GCE) was introduced. This complex is a Schiff base complex and is used as a modifier to enhance the electrochemical operation of a non-enzymatic sensor to determine glucose. The reasons for using this specific complex in this work are because of the advantages of Ni complexes, such as catalytic activity, selectivity, stability and cost-effectiveness [19,21,23,24]. The performance of the electrochemical sensor was investigated by different electrochemical methods. They are cyclic voltammetry (CV), differential pulse voltammetry (DPV), chronoamperometry (CA), and electrochemical impedance spectroscopy (EIS).

Experimental

Chemicals

The employed materials were of analytical grades. Amino ethyl ethanol amine (AEEA), benzoyl acetone (BZA), $Ni(NO_3)_2{\cdot}6H_2O$, methanol, potassium thiocyanate (KSCN), sodium hydroxide (NaOH), glucose ($C_6H_{12}O_6$), ascorbic acid (AA), uric acid (UA), fructose (Fru), citric acid (CA), dopamine (DA) and sucrose were bought from Merck (Darmstadt, Germany). All solutions were made with distilled water.

Preparation of [Ni(HL)NCS] modifier

To synthesize the modifier, the ligand solution was first prepared by combining similar amounts of AEEA (0.001 mol) and BZA (0.001 mol) in 30 mL methanol under reflux for 2 hours. The resulting bright yellow solution, including the ligand (HL = aminoethylethanolaminebenzoylacetone) was applied for complex synthesis. Then, $Ni(NO_3)_2{\cdot}6H_2O$ (0.001 mol) was added to this ligand solution and stirred for 1 hour, when a solution of KSCN (0.097 g in 3 mL water) was added and stirred for another 1 hour. The colour of the solution changes to brown. The obtained suspension was filtered and put aside until it became crystalline. Red-yellow needle crystals appeared by slow solvent evaporation at room temperature and filtered, washed with ethanol, and dried [25].

Fabrication of MR-NiC/GCE

The GCE surface (diameter = 2 mm, A = 0.0314 cm^2) was polished by alumina slurry. 5 µL of modifier solution (3 mg mL^{-1}), [Ni(HL)NCS] in DIW/ethanol, was cast on the GCE surface by drop-casting method and dried in air.

Physicochemical and electrochemical measurements

The synthesized modifier (complex sample) was characterized using field-emission scanning electron microscopy (FE-SEM) coupled with energy-dispersive X-ray spectroscopy (EDS), examined by ZEISS sigma 300-HV (Germany). Fourier transform infrared (FT-IR) spectroscopy analysis was examined by Bruker equinox 55 (USA) in the wavenumber range from 400 to 4000 cm^{-1}.

All electrochemical tests were performed by potentiostat/galvanostat (RADstat-1A, Iran) made by Kian Shar Danesh with the Ivium software package at room temperature using a three-electrode system. The MR-NiC/GCE was utilized as a working electrode, Ag/AgCl/KCl (3M) as a reference electrode, and Pt electrode as a counter electrode. Most of the electrochemical measurements were done in 0.1 M NaOH solution at a potential scan rate of 50 mV s^{-1} over the potential window of 0.2 to 0.7 V *vs.* Ag/AgCl.

Results and discussion

Structure and morphology characterizations of synthesized modifier

FT-IR characterization revealed the functional groups in the synthesized modifier structure (Figure 1a). The acquired peaks at 3423, 3252 and 2926 cm^{-1} are related to OH stretching, N-H bending, and CH stretching, respectively. The peak at 2110 cm^{-1} is related to SCN and at 1626 cm^{-1} is related to C=O. The peaks at 1603 and 1511 cm^{-1} indicate the C=C of the aromatic ring. The peak at 1603 cm^{-1} is for overlapping of C=N with C=C band. The peaks at 1381, 1128 and 1064 cm^{-1} correspond to the bending C-H, the stretching CN, and C-O, respectively.

The results of the EDS analysis are shown in Figure 1b, which confirms the presence of the elements in the modifier structure (Ni = 10.34 wt.%, C = 44.32 wt.%, S = 5.45 wt.%, N = 15.43 wt.%, O = 24.46 wt.%). Figure 1c and Figure 1d represent the FE-SEM images of the modifier with different magnifications. The recorded images show the micro-rod structure of the modifier along with determining the thickness of the micro-rods. In the EDS layered image, the distribution of elements is shown with different colours (Figure 1e). Also, the distribution of each element is shown separately in the elemental mapping figures, which show the homogeneous distribution of the elements (Figure 1f-j).

Electrolytic oxidation of glucose

Optimization of NaOH concentration and modifier amount

In order to select the appropriate electrolyte solution, a phosphate buffer solution (0.1 M) with various pH values (2-13) was examined. A weak CV oxidation peak was observed only in the buffer with pH 13. This is because glucose is less active in acidic environments, and its oxidation is easier in alkaline environments. Complex-based glucose sensors operate more easily in a high pH value because they need the presence of hydroxide ions (OH^-) to oxidize glucose molecules [18]. NaOH is usually utilized as an electrolyte in non-enzymatic glucose sensors [26-28]. In this work, we used NaOH solution as an electrolyte. To optimize the concentration of NaOH, CV voltammograms are recorded in different concentrations of NaOH from 0.01 to 1 M in the absence and presence of glucose, and results are presented in Figure S1 of the Supplementary material. The concentration of 0.1 M with a higher current was selected as the optimum concentration. A shift of the oxidation potential towards more positive potentials at lower concentrations of NaOH indicates that the activity of glucose is higher in an alkaline solution. Also, an increment in current was observed in the presence of glucose at all concentrations (Supplementary material, Figure S1).

In order to optimize the concentration of the modifier, different concentrations from 1 to 9 mg mL^{-1} were used to record CV voltammograms in 0.1 M NaOH solution in the absence and presence of glucose. It is seen in Figure S2 that the highest current was recorded at 3 mg mL^{-1}. Also, different amounts of modifier drop casting on the GCE surface from 1 to 6 µL with an optimal concentration of 3 mg mL^{-1} were investigated using the CV method in 0.1 M NaOH solution in the absence and presence of glucose. The amount of 5 µL showed the highest current and was considered optimum (Figure S3)

Cyclic voltammetry of bare and optimized MR-NiC/GCE

To investigate electrochemical performance, CV measurements were performed at a bare GCE and the optimized MR-NiC/GCE in 0.1 M NaOH solution at v = 50 mV s^{-1} with the presence of glucose and without it (Figure 2).

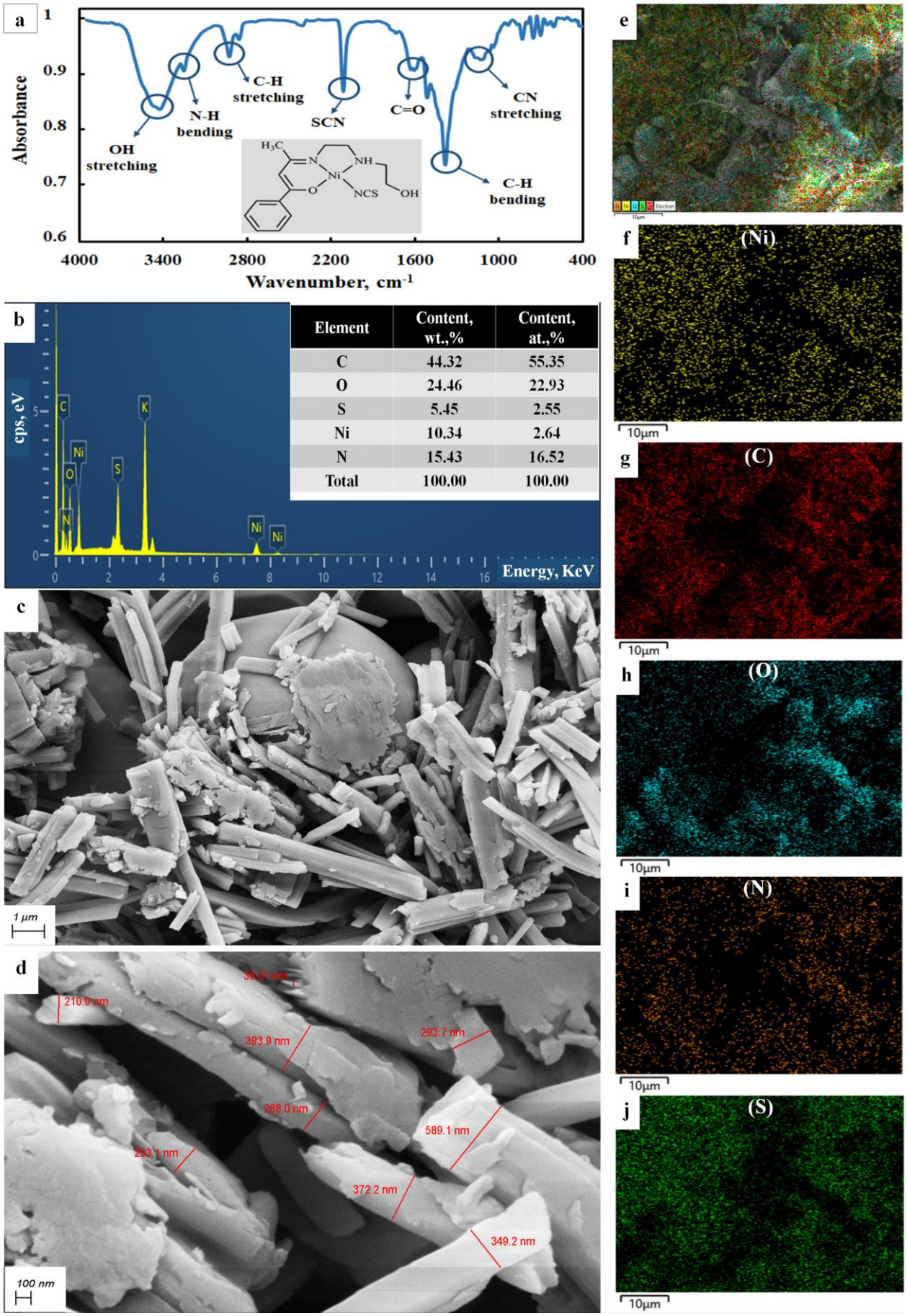

Figure 1. *Surface characterization of synthesized modifier: (a) FT- IR spectrum, (b) EDS spectrum, (c, d) FE-SEM images at different magnifications, (e) EDS layered image, (f-j) EDS elemental mapping images of Ni, C, O, N, and S, respectively*

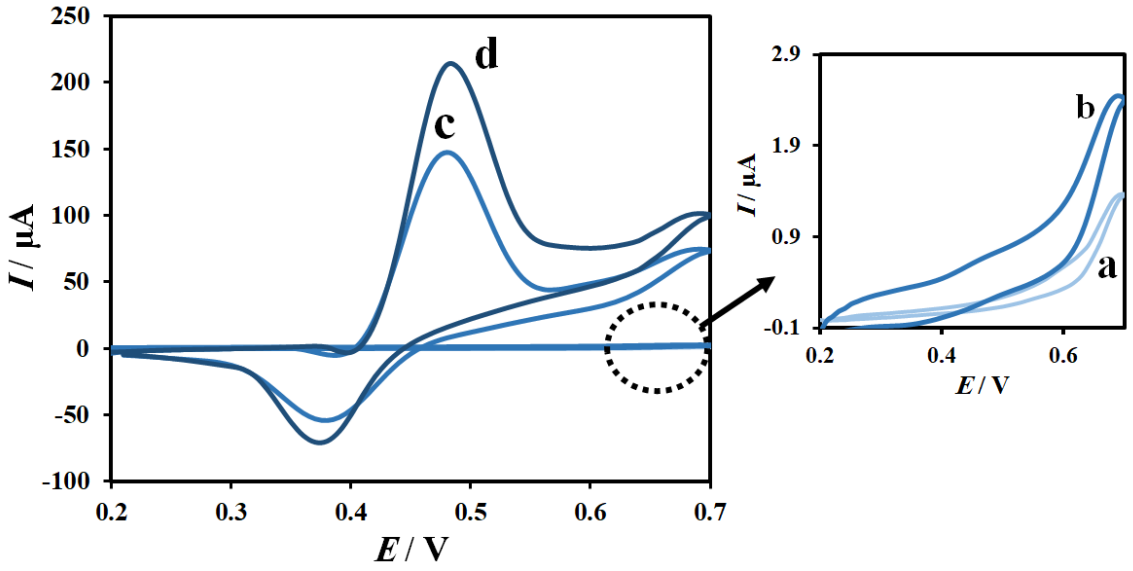

Figure 2. *CV voltammograms (50 mV s^{-1}) in 0.1 M NaOH of bare GCE in (a) absence of glucose, (b) with 1.0 mM glucose, and optimized MR-NiC/GCE in (c) absence of glucose, (d) with 1.0 mM glucose*

The bare GCE did not show any peak in the absence and presence of glucose (Figure 2a, b), while the optimized MR-NiC/GCE showed peaks in either blank solution or in the presence of glucose (Figure 2c, d). According to the recorded voltammograms, the potential of the anodic and cathodic peaks for the MR-NiC/GCE is at 0.48 and 0.38 V, respectively (Figure 2c). The peak separation is $\triangle E_p$ = 0.1 V, higher than 59/*n* mV (*n* = 1) for the reversible system. Therefore, the system is quasi-reversible. Also, the MR-NiC/GCE indicates a current that is increased in the presence of glucose (Figure 2d), which reveals the acceptable performance of the modified electrode to detect glucose and its oxidation. This can be attributed to the presence of nickel in the structure of the modifier [27-29], which can oxidize glucose in an alkaline medium according to the following mechanism:

$$Ni(II)L \rightarrow Ni(III)L + e^- \quad (1)$$

$$Ni(III)L + Glucose \rightarrow Ni(II)L + Gluconolactone \quad (2)$$

The redox peak observed in the absence of glucose (Figure 2c) is attributed to the conversion of Ni(II)L to Ni(III)L and *vice versa*. Ni(II)L is the Ni ion present in the modifier structure. In the presence of glucose, the anodic peak in Figure 2d increases significantly. The potential peak for glucose oxidation coincides well with the oxidation of Ni(II)L to Ni(III)L. These findings indicate the active involvement of the Ni complex in the electrochemical oxidation of glucose.

To understand the effect of scan rate on the electrochemical performance of the sensor and calculate kinetic parameters, the optimized MR-NiC/GCE was utilized to record CV voltammograms in 0.1 M NaOH solution at different scan rates from 5 to 2100 mV s^{-1}. MR-NiC/GCE was placed in NaOH solution (0.1 M) without glucose and in the presence of 1 mM glucose. Results in Figure 3a-d are related to the absence of the analyte, while these in Figure 3e-g to the presence of the analyte.

According to Figure 3a, with increment of scan rate (5.00, 10.0, 25.0, 50.0, 100, 200, 300, 400, 500, 600, 700, 800, 900, 1000, 1100, 1200, 1300, 1400, 1500, 1600, 1700, 1800, 1900, 2000 and 2100 mV s^{-1}), the anodic and cathodic currents increased and also the peak separation ($\triangle E_p$), what indicates the kinetic limitation of charge transfer at high scan rates. At lower scan rates, the peak separation is independent of the scan rate as a result of fast charge transfer kinetics between the modifier and the electrode surface.

The kinetic parameters such as anodic and cathodic transfer coefficients (α_a) and (α_c), apparent charge transfer rate constant (k_s), and modified electrode surface coverage (Γ) can be estimated. To calculate the surface coverage of the MR-NiC/GCE, the slope of the anodic currents plot *versus* scan rates (Figure 3b) and equation (3) were used [30].

$$I_p=n^2F^2A\Gamma v/4RT \quad (3)$$

For n = 1 and A = 0.0314 cm^2, the amount of surface coverage (Γ) was calculated as 14.1 nmol cm^{-2}. To calculate the apparent charge transfer rate constant (k_s) based on Laviron's equation, the condition $\triangle E_p \geq 200/n$ mV is necessary [31]. According to Figure 3c, d, this condition is attained at 600 mV s^{-1} and higher scan rates. Using Laviron's equation (4) [30], the k_s value was calculated for the scan rates of 600 mV s^{-1} and above.

The Laviron equation describes the relationship between the potential and current in electrochemical processes, particularly focusing on the kinetics of electron transfer mechanisms. In equation (4), v is the scan rate and n is the number of electrons involved in the overall redox reaction of the modifier, and all other symbols have their usual meanings. The average of the k_s value was calculated as 1.52 s^{-1}. The redox transfer coefficients were obtained 0.6 and 0.4 (for n_α = 1, using the slope of the plot (Figure 3d) and the equations (5) and (6).

$$\log k_s = \alpha \log (1-\alpha) + (1-\alpha) \log \alpha - \log (RT/nFv) - \alpha (1- \alpha) n_\alpha F\triangle E_p/2.3RT \quad (4)$$

$$\text{Slope}_a = 2.3RT/(1-\alpha) n_\alpha F \quad (5)$$

$$\text{Slope}_c = -2.3RT/\alpha n_\alpha F \quad (6)$$

In order to investigate the kinetics of electrochemical glucose oxidation, CV experiments were performed at different scan rates using optimized MR-NiC/GCE in 0.1 M NaOH containing 1 mM glucose. Figure 3e indicates an increment in oxidation peak and reduction peak currents with the increment in the scan rate. Furthermore, the oxidation peak potential moved toward positive values, while the reduction peak potential shifted toward negative values, and the potential difference (ΔE_p) between these potentials is enhanced. This happens because, at higher scan rates, the electrode needs a higher overpotential to acquire a similar electron transfer rate [32]. The obtained oxidation and reduction peak currents in CV voltammograms are illustrated versus the square root of scan rates in Figure 3f, where a linear relationship can be seen, indicating that the MR-NiC/GCE recognized glucose oxidation as an electrochemical process controlled by diffusion [32]. The Tafel plot was drawn from the Tafel area at v = 10 mV s^{-1} (Figure 3g). Using the slope of the Tafel plot (0.0435) defined by equation (5) and n_α = 1, the electron transfer coefficient between glucose and MR-NiC/GCE surface was calculated as 0.36.

Differential pulse voltammetry and chronoamperometry of MR-NiC/GCE sensor

The differential pulse voltammetry (DPV) method was employed to study the electrochemical performance of glucose oxidation on the surface of the MR-NiC/GCE and to determine the limit of detection (LOD) and linear dynamic range (LDR) values for the introduced sensor. For this purpose, the MR-NiC/GCE was investigated in 0.1 M NaOH solution, including various concentrations of glucose with the DPV technique (Figure 4a). According to the calibration curve (Figure 4b), the current rises linearly with the glucose concentration, and the LDR value is 100-1100 µM. Note that the background current (the current in the absence of glucose related to the oxidation of the Ni complex on the surface) was subtracted from the recorded current, and the calibration curve given in Figure 4b is based only on the oxidation current of glucose. Subtracting the background current helps to isolate the signal due to the analyte, thus allowing a more accurate determination of its concentration. This ensures that the calibration curve reflects only the response attributable to the glucose.

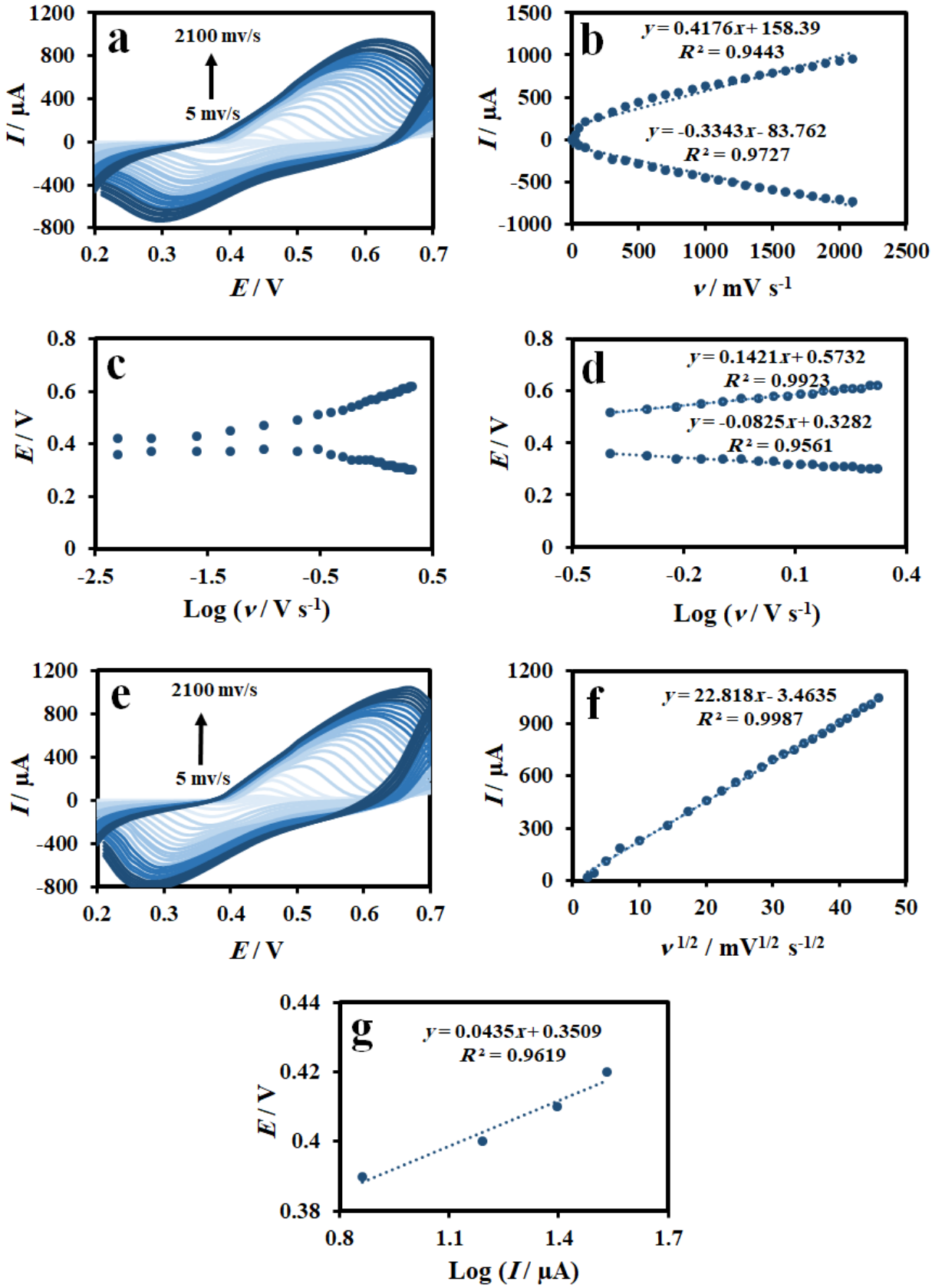

Figure 3. *(a) CV voltammograms of MR-NiC/GCE in 0.1 M NaOH solution (blank) at various scan rates from 5.00 to 2100 mV s^{-1}, (b) anodic and cathodic peak current plots versus scan rate, (c) anodic and cathodic peak potential changes versus logarithm of scan rates, (d) magnified linear parts of plot c, (e) CV voltammograms of MR-NiC/GCE in 0.1 M NaOH solution in the presence of 1 mM glucose at various scan rates from 5.00 to 2100 mV s^{-1}, (f) oxidation peak current plot versus square root of scan rates, (g) Tafel plot from the Tafel region at ν = 10 mV s^{-1}*

To estimate the LOD value, several DPV voltammograms were recorded for the MR-NiC/GCE in the absence of glucose (blank solution) and the standard deviation (S) for recorded voltammograms was calculated. By the slope of the calibration curve (m) and the (LOD = $3S_b/m$) equation, the LOD value was calculated as 15.8 µM.

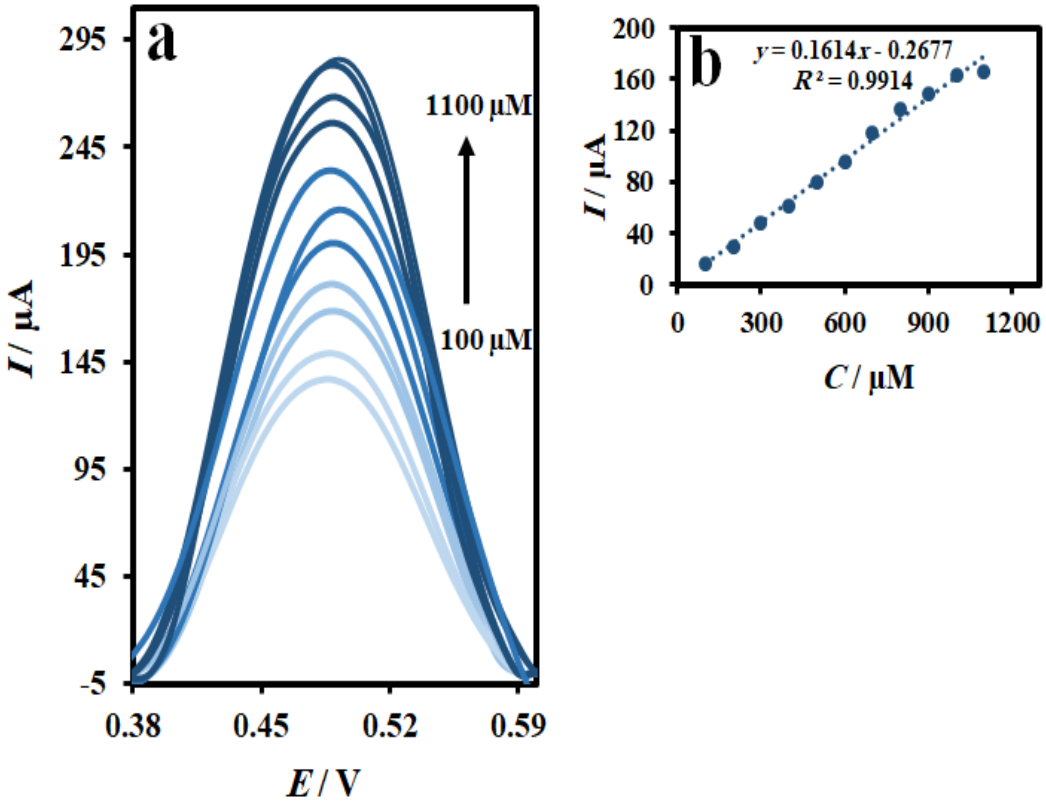

Figure 4. *(a) DPV voltammograms for MR-NiC/GCE in 0.1 M NaOH solution including various concentrations of glucose: 100, 200, 300, 400, 500, 600, 700, 800, 900, 1000, 1100 µM at* ν *= 50 mV* s^{-1}*, (b) calibration curve*

In order to examine the electrochemical performance of glucose oxidation at the MR-NiC/GCE, the chronoamperometry (CA) method was also used. For this part, 0.1 M NaOH solution, including different concentrations of glucose was prepared, and chronoamperometric studies were done using a potential step (0.53 V) for 25 seconds. According to the results shown in Figure 5a, chronoamperometric current is enhanced with the increment of glucose concentrations, and the current decreases with time and reaches a steady state. In order to calculate the diffusion coefficient D, the diagram of the current versus $t^{-1/2}$ for each glucose concentration was drawn in Figure 5b. The slopes of the resulting curves were used to draw Figure 5c. Using the Cottrell equation that demonstrates the dependence of the current on the concentration and the slope of the plot in Figure 5c, the D value for glucose was calculated (D = 5.45×10^{-5} cm^2 s^{-1}) [33].

Electrochemical impedance spectroscopy

Electrochemical impedance spectroscopy was used to investigate the effect of the modifier on the performance of the GCE, the surface coating, and also the electron transfer between the electrode surface and electrolyte. A solution of 0.1 M KCl containing 5 mM $[Fe(CN)_6]^{-3/-4}$ was used and EIS measurements were performed in the frequency range of 100000–0.1 Hz. As can be seen from the Nyquist plots presented in Figure 5d, the charge transfer resistance (R_{ct}) of the bare GCE is 497 and 1502 Ω for the MR-NiC/GCE. The increase in the value of R_{ct} by 1005 Ω indicates good coverage of the modifier on the surface of the GCE. The increase in charge transfer resistance on the surface of the

MR-NiC/GCE is due to the electrostatic repulsion created between the redox probe $[Fe(CN)_6]^{3-/4-}$ and the modifier [Ni(HL)NCS] (having a negative surface charge) [25]. Therefore, according to the investigations, the MR-NiC/GCE provides the active surface and surface coating suitable for glucose measurement. The prepared electrode facilitates the process of glucose oxidation on the electrode surface due to the structure of the modifier and the active nickel redox nuclei in it. To better compare the results, the CV voltammograms of bare GCE and MR-NiC/GCE in the above solution were recorded. According to the results of Figure 5e, the current on the modified electrode decreased by 18 µA. This evidence confirms the results obtained from the Nyquist plot well.

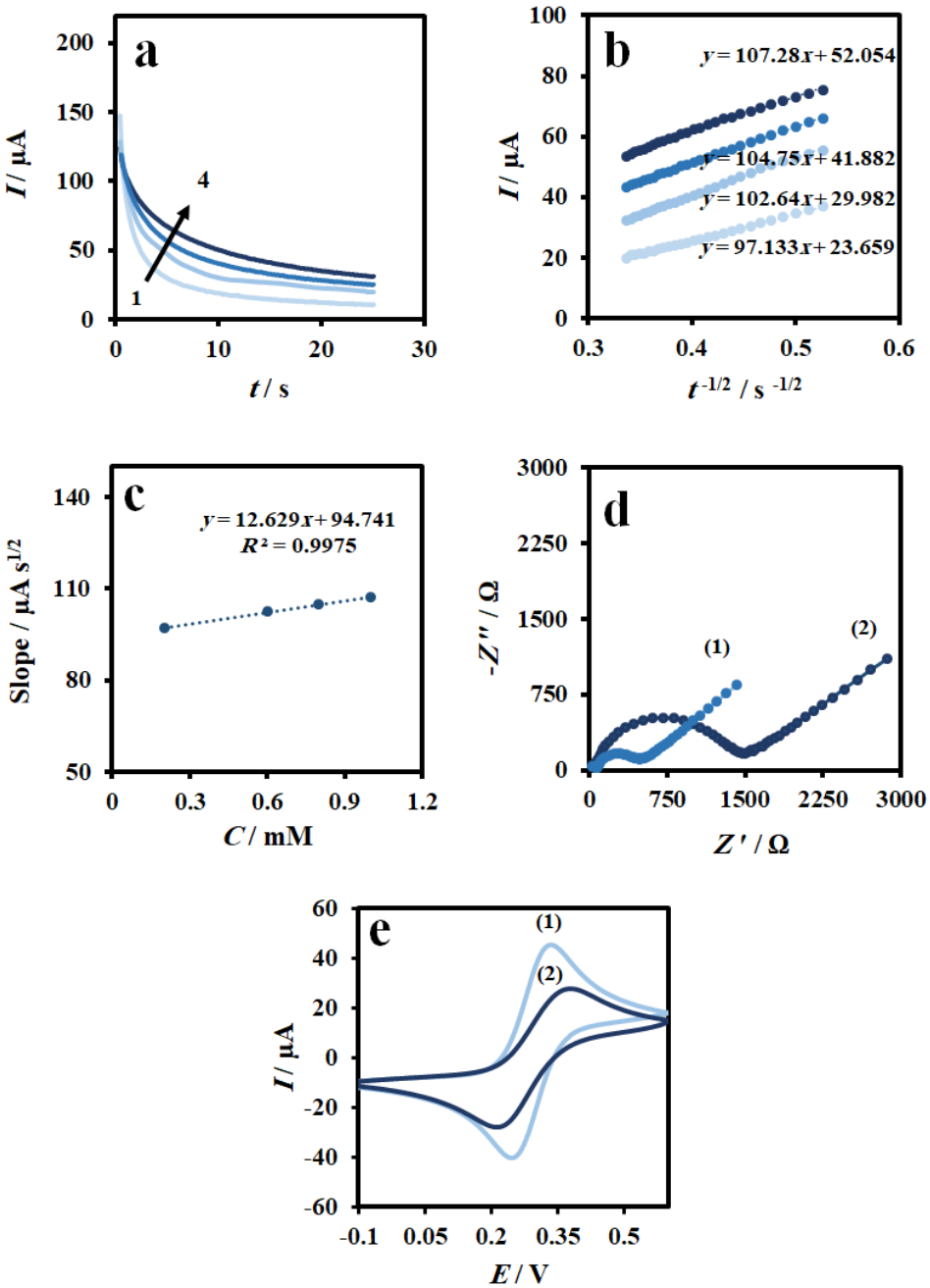

Figure 5. *(a) Chronoamperograms of MR-NiC/GCE in 0.1 M NaOH solution with various concentrations of glucose from 1 to 4, respectively: 0.20, 0.60, 0.80 and 1.0 mM by applying a potential step of 0.53 V, (b) the plot of current versus ($t^{-1/2}$) for concentrations 1 to 4, (c) slope diagram of the lines resulting from diagram b versus glucose concentration, (d) Nyquist plots of bare GCE (1) and MR-NiC/GCE (2) in 0.1 M KCl containing 5 mM $[Fe(CN)_6]^{-3/-4}$ solution in the frequency range of 100000 to 0.1 Hz and the potential of 0.3 V, (e) CV voltammograms of bare GCE (1) and MR-NiC/GCE (2) in 0.1 M KCl containing 5 mM $[Fe(CN)_6]^{-3/-4}$ solution at ν = 50 mV s^{-1}*

Stability, reproducibility, repeatability, and anti-interference of MR-NiC/GCE sensor

The long-term stability of the electrodes is a significant factor in finding whether the electrodes have a potential application. For this purpose, the electrochemical signals of the MR-NiC/GCE were measured in the NaOH solution involving glucose (1 mM) using the DPV technique from one week to 2 weeks. Then, the modified GCE was placed at room temperature. The results are shown in Figure S4, a. The current response after two weeks remained at 55.2 % of the initial current response. It is a good long-term stability.

The reproducibility of the introduced sensor was explored by measuring the current responses in the 0.1 M NaOH solution containing 1 mM glucose by five independent electrodes prepared under similar conditions. As can be seen in Figure S4 b, DPV measurements showed a relative standard deviation (RSD) of 2.5 % for the current, confirming a good reproducibility of MR-NiC/GCE. The repeatability was examined using DPV for measuring glucose with the MR-NiC/GCE. The five repeated measurements were performed (Figure S4, c). The RSD value was 1.5 %. It confirms proper repeatability. Also, the cycling stability of the MR-NiC/GCE was investigated using the CV method. According to the results presented in Figure S5, during the recording of 50 consecutive cycles at v = 50 mV s^{-1}, a change of less than 5 % in current is observed, which suggests excellent cycling stability for the modifier on the surface of the GCE. Another important problem for non-enzymatic sensors is the interference of other materials in the blood due to their oxidization at the same potential as glucose. To study the effect of interference and selectivity of the designed sensor, it is necessary to investigate the effect of various concentrations of interfering species in the presence of glucose using DPV. For this purpose, different concentrations of interfering species were added to the solution and checked by MR-NiC/GCE. All interfering species were examined in 0.1 M NaOH solution involving 0.3 mM glucose. The interfering species were dopamine, fructose, uric acid, citric acid, ascorbic acid, and sucrose. Results confirm the great selectivity of the designed sensor (Table S1).

Glucose measuring in human blood serum

To study the efficiency of the sensor for measuring glucose in real samples, the MR-NiC/GCE was utilized to determine glucose in human blood serum samples prepared from a medical laboratory. DPV and standard addition methods were used for this part. To do this experiment, a constant amount of blood sample (100 µL) was added to each of the five volumetric flasks (10 mL). Then, 0, 2, 4, 6 and 8 µL of 0.5 M standard glucose solution were added. Finally, all the flasks were brought to a volume of 10 mL using NaOH (0.1 M). The current of each solution was recorded using DPV. The calibration curve was drawn for each sample (1, 2, 3), and the unknown glucose concentration values were obtained by extrapolation the diagrams (Figure S6). Here, background currents (currents related to the oxidation of the complex on the surface) were also subtracted from the recorded currents. Table 1 compares different results (RSD, recovery, error percent, *t*-test, *etc*.) for samples. These results show that the proposed sensor displays acceptable accuracy for measuring glucose. A comparison of the introduced electrode and some non-enzymatic glucose sensors is given in Table 2. According to this comparison, the proposed non-enzymatic sensor indicates better LOD than others [34-43].

Table 1. *Glucose measuring in human blood serum (3 samples, N=4)*

Plasma sample	Claimed glucose concentration, mM	Founded glucose concentration, mM	Recovery, %	Error, %	RSD, % N = 4	*t*-test
1	14.82	14.54 ±0.29	98.11	-1.89	1.99	1.93
2	11.27	11.04 ±0.25	97.95	-2.05	2.26	1.84
3	5.05	5.12 ±0.16	101.38	+1.38	3.12	0.87

Table 2. *Comparison of analytical performance of the sensor designed in the present work for glucose measurement with some other designed sensors*

Modifier	LOD, µM	LDR, mM	Electrolyte	Ref.
Pt NFs[1]	48	1-16	0.1 M NaOH	[34]
3D porous Au-graphene	25	0.1-2	0.1 M PBS	[35]
Pd/Au cluster	50	0.1-30	0.1 M NaOH	[36]
Pt-C NF[2]	33	0.3-17	0.1 M NaOH	[37]
Cu/CuO/$Cu(OH)_2$	20	0-20	0.1 M NaOH	[38]
Cu nanowires	35	0-3	0.1 M NaOH	[39]
Pt Film/Cu foam	385	1-11	0.1 M PBS	[40]
ZrO_2-Cu(I)	250	1-10	0.1 M NaOH	[41]
Co_7Fe_3/NPCSs[3]	401	0.001-2.2	0.1 M NaOH	[42]
MnO_2MWCNT[4]	53	0.5-4.4	0.5 M NaOH	[43]
MR-NiC	15.8	0.1-1.1	0.1 M NaOH	This work

[1]Platinum nanoflowers; [2]Carbon fiber supported platinum nanoparticles; [3]Co_7Fe_3 nanoparticles coupled with nitrogen-doped porous carbon nanosheets; [4]Multiwalled carbon nanotube

Conclusions

In this research, an electrochemical sensor was constructed by a glassy carbon electrode modified using micro-rods nickel-based complex ([Ni(HL)NCS]) as a novel modifier for glucose detection. According to the results, this modifier has good stability on the electrode surface and covers its surface well. Due to the presence of nickel, the modifier facilitates the process of glucose oxidation on the electrode surface and can oxidize glucose in an alkaline environment. This sensor was utilized to determine glucose in human blood serum, and the measurement results were not significantly different from the medical laboratory results. This sensor indicated a good LDR value of 100 to 1100 µM and an excellent LOD value of 15.8 µM (*S*/*N* = 3), along with a significant anti-interfering performance and high stability that makes it attractive as a kind of promising non-enzymatic sensor for practical glucose detecting.

Supplementary material: *Additional data are available electronically on article page of the journal's website: https://pub.iapchem.org/ojs/index.php/JESE/article/view/2368, or from the corresponding author upon request.*

Acknowledgement: *The authors gratefully acknowledge the financial support provided by the Yazd University Research Council for this research.*

References

[1] M. A. Ghaffarirad, A. Sabahi, Z. Golshani, F. Manteghi, A. Ghaffarinejad, Non-enzymatic glucose electrochemical sensor based on nitrogen-doped graphene modified with polyaniline and Fe_3O_4@MIL-101-NH_2 nano framework, *Inorganic Chemistry Communications* **159** (2024) 111812. https://doi.org/10.1016/j.inoche.2023.111812

[2] S. Mohajeri, A. Dolati, K. Yazdanbakhsh, Synthesis and characterization of a novel non-enzymatic glucose biosensor based on polyaniline/zinc oxide/multi-walled carbon nanotube ternary nanocomposite, *Journal of Electrochemical Science and Engineering* **9** (2019) 207-222. https://doi.org/10.5599/jese.666

[3] T. Yang, W. Zhang, J. Wu, C. Zhang, Y. Song, Y. Zhao, Programming a triple-shelled CuS@$Ni(OH)_2$@CuS heterogeneous nanocage as robust electrocatalysts enabling long-term highly sensitive glucose detection, *Electrochimica Acta* **438** (2023) 141588. https://doi.org/10.1016/j.electacta.2022.141588

[4] L. Tang, S.J. Chang, C.-J. Chen, J.-T. Liu, Non-invasive blood glucose monitoring technology: A review, *Sensors* **20** (2020) 6925. https://doi.org/10.3390/s20236925

[5] Y. Xue, A.S. Thalmayer, S. Zeising, G. Fischer, M. Lübke, Commercial and Scientific Solutions for Blood Glucose Monitoring—A Review, *Sensors* **22** (2022) 425. https://doi.org/10.3390/s22020425

[6] A. Venkadesh, J. Mathiyarasu, S. Dave, S. Radhakrishnan, Amine mediated synthesis of nickel oxide nanoparticles and their superior electrochemical sensing performance for glucose detection, *Inorganic Chemistry Communications* **131** (2021) 108779. https://doi.org/10.1016/j.inoche.2021.108779

[7] M. Mazloum-Ardakani, Z. Mokari, Z. Alizadeh, H. Mohammadian-Sarcheshmeh, M. Abdollahi-Alibiek, B.B.F. Mirjalili, N. Salehi, Electrochemical sensor for sensitive detection of an anticancer drug Capecitabine by modified carbon paste electrode with tetrahydrodipyrazolo pyridine derivative and Cu-MCM-41 nanoparticles, *Microchemical Journal* **199** (2024) 109887. https://doi.org/10.1016/j.microc.2023.109887

[8] N. Sahraei, M. Mazloum-Ardakani, F. Hoseynidokht, Electrochemical paper-based biosensors for point-of-care diagnostics: Detection methods and applications, *Journal of Electrochemical Science and Engineering* **12** (2022) 399-419. https://doi.org/10.5599/jese.1104

[9] M. Mazloum-Ardakani, F. Alvansaz-Yazdi, F. Hosseini-Dokht, A. Khoshroo, Fabrication of an Electrochemical Sensor for Determination of Epinephrine Using a Glassy Carbon Electrode Modified with Catechol, *Analytical and Bioanalytical Chemistry Research* **10** (2023) 387-394. https://doi.org/10.22036/abcr.2023.386655.1889

[10] M. Mazloum-Ardakani, Z. Tavakolian-Ardakani, N. Sahraei, S.M. Moshtaghioun, Fabrication of an ultrasensitive and selective electrochemical aptasensor to detect carcinoembryonic antigen by using a new nanocomposite, *Biosensors and Bioelectronics* **129** (2019) 1-6. https://doi.org/10.1016/j.bios.2018.12.047

[11] M. Mazloum-Ardakani, N. Sadri, V. Eslami, Detection of Dexamethasone Sodium Phosphate in Blood Plasma: Application of Hematite in Electrochemical Sensors, *Electroanalysis* **32** (2020) 1148-1154. https://doi.org/10.1002/elan.201900498

[12] M. Hasanzadeh, Z. Hasanzadeh, S. Alizadeh, M. Sayadi, M.N. Nezhad, R.E. Sabzi, S. Ahmadi, Copper-nickel oxide nanofilm modified electrode for non-enzymatic determination of glucose, *Journal of Electrochemical Science and Engineering* **10** (2020) 245-255. https://doi.org/10.5599/jese.699

[13] M. Chen, C. Wang, F. Chen, H. Li, Y. Wang, H. Ma, Exploiting synergistic interaction in Cu-Zn-Ni alloy oxide films prepared by one-step anodizing for a highly sensitive non-enzymatic glucose sensor, *Inorganic Chemistry Communications* **157** (2023) 111278. https://doi.org/10.1016/j.inoche.2023.111278

[14] W. Han, X. Zhang, R. Wang, T. Bai, H. Liu, L. Cui, J. Liu, X. Liang, Non-enzymatic electrochemical glucose sensor based on Pt2Pd1 alloy nanocrystals with high-index facets, *Journal of Alloys and Compounds* **936** (2023) 168287. https://doi.org/10.1016/j.jallcom.2022.168287

[15] L. Shahhoseini, R. Mohammadi, B. Ghanbari, S. Shahrokhian, Ni(II) 1D-coordination polymer/C 60 -modified glassy carbon electrode as a highly sensitive non-enzymatic glucose electrochemical sensor, *Applied Surface Science* **478** (2019) 361-372. https://doi.org/10.1016/j.apsusc.2019.01.240

[16] Q. Dong, H. Ryu, Y. Lei, Metal oxide based non-enzymatic electrochemical sensors for glucose detection, *Electrochimica Acta* **370** (2021) 137744. https://doi.org/10.1016/j.electacta.2021.137744

[17] H. Zhu, L. Li, W. Zhou, Z. Shao, X. Chen, Advances in non-enzymatic glucose sensors based on metal oxides, *Journal of Materials Chemistry B* **4** (2016) 7333-7349. https://doi.org/10.1039/C6TB02037B

[18] A. D. Daud, H. N. Lim, I. Ibrahim, N. A. Endot, N. S. K. Gowthaman, Z. T. Jiang, K. E. Cordova, An effective metal-organic framework-based electrochemical non-enzymatic glucose sensor, *Journal of Electroanalytical Chemistry* **921** (2022) 116676. https://doi.org/10.1016/j.jelechem.2022.116676

[19] M. Mazloum-Ardakani, E. Amin-Sadrabadi, A. Khoshroo, Enhanced activity for non-enzymatic glucose oxidation on nickel nanostructure supported on PEDOT:PSS, *Journal of Electroanalytical Chemistry* **775** (2016) 116-120. https://doi.org/10.1016/j.jelechem.2016.05.044

[20] D. M. González, L. A. Hernández, J. Oyarce, A. Alfaro, N. Novoa, J. Cisterna, I. Brito, D. Carrillo, C. Manzur, A new and efficient high-performance electrochemical glucose sensor based on a metallopolymer derived from a cobaltate (III) Schiff base complex, *Synthetic Metals* **271** (2021) 116633. https://doi.org/10.1016/j.synthmet.2020.116633

[21] M. Revenga-Parra, S. N. Robledo, E. Martínez-Periñán, M. M. González-Quirós, A. Colina, A. Heras, F. Pariente, E. Lorenzo, Direct determination of monosaccharides in honey by coupling a sensitive new Schiff base Ni complex electrochemical sensor and chemometric tools, *Sensors and Actuators, B: Chemical* **312** (2020) 127848. https://doi.org/10.1016/j.snb.2020.127848

[22] Z. Deng, H. Long, Q. Wei, Z. Yu, B. Zhou, Y. Wang, L. Zhang, S. Li, L. Ma, Y. Xie, J. Min, High-performance non-enzymatic glucose sensor based on nickel-microcrystalline graphite-boron doped diamond complex electrode, *Sensors and Actuators B: Chemical* **242** (2017) 825-834. https://doi.org/10.1016/j.snb.2016.09.176

[23] M. Rezaeinasab, A. Benvidi, M. D. Tezerjani, S. Jahanbani, A. H. Kianfar, M. Sedighipoor, An Electrochemical Sensor Based on Ni(II) Complex and Multi Wall Carbon Nano Tubes Platform for Determination of Glucose in Real Samples, *Electroanalysis* **29** (2017) 423-432. https://doi.org/10.1002/elan.201600162

[24] M. A. Sultan, S. S. Hassan, K. A. Omran, H. B. Hassan, A novel Ni-Schiff base complex for motivating glucose electrooxidation in alkaline solutions, *Materials Advances* **5** (2024) 1264-1283. https://doi.org/10.1039/d3ma00730h

[25] R. Vafazadeh, S. Aghayani, A. C. Willis, Synthesis, structure characterization and Hirshfeld surface analysis of Ni(II) complexes with a flexidentate ligand: a dinuclear complex with O−H−O bond, *Journal of Molecular Structure* **1246** (2021) 131192. https://doi.org/10.1016/j.molstruc.2021.131192

[26] Q. Q. Sun, M. Wang, S. J. Bao, Y. C. Wang, S. Gu, Analysis of cobalt phosphide (CoP) nanorods designed for non-enzyme glucose detection, *Analyst* **141** (2016) 256-260. https://doi.org/10.1039/c5an01928a

[27] M. Wei, Y. Qiao, H. Zhao, J. Liang, T. Li, Y. Luo, S. Lu, X. Shi, W. Lu, X. Sun, Electrochemical non-enzymatic glucose sensors: recent progress and perspectives, *Chemical Communications* **56** (2020) 14553-14569. https://doi.org/10.1039/d0cc05650b

[28] P. K. Sonkar, V. Ganesan, S. A. John, D. K. Yadav, R. Gupta, Non-enzymatic electrochemical sensing platform based on metal complex immobilized carbon nanotubes for glucose determination, *RSC Advances* **6** (2016) 107094-107103. https://doi.org/10.1039/c6ra16064f

[29] T. Zhe, X. Sun, Y. Liu, Q. Wang, F. Li, T. Bu, P. Jia, Q. Lu, J. Wang, L. Wang, An integrated anode based on porous Ni/$Cu(OH)_2$ nanospheres for non-enzymatic glucose sensing, *Microchemical Journal* **151** (2019) 104197. https://doi.org/10.1016/j.microc.2019.104197

[30] M. Mazloum-Ardakani, H. Mohammadian-Sarcheshmeh, A. Khoshroo, M. Abdollahi-Alibeik, Thiosemicarbazide derivative-functionalized carbon nanotube for simultaneous determination of isoprenaline and piroxicam, *Journal of Analytical Science and Technology* **8** (2017) 6. https://doi.org/10.1186/s40543-017-0115-z

[31] M. Mazloum-Ardakani, F. Jokar, H. Mohammadian-Sarcheshmeh, B. B. F. Mirjalili, S. S. Hosseinikhah, Electrochemical Behavior of Benzoxanthene Compound in Modified Glassy Carbon Electrode by Zinc Sulfide Particles Warped in CNT/RGO Nanosheets for Determination of Hydrazine, *Iranian Journal of Analytical Chemistry* **8** (2021) 15-24. https://doi.org/10.30473/ijac.2021.60559.1208

[32] Y. Kang, X. Ren, Y. Li, Z. Yu, Ni-Coated Diamond-like Carbon-Modified TiO_2 Nanotube Composite Electrode for Electrocatalytic Glucose Oxidation, *Molecules* **27** (2022) 5815. https://doi.org/10.3390/molecules27185815

[33] A. J. Bard, L. R. Faulkner, *Electrochemical Methods: Fundamentals and Applications, second ed.,* John Wiley & Sons, New York, 2001.

[34] M. Q. Guo, H. S. Hong, X. N. Tang, H. D. Fang, X. H. Xu, Ultrasonic electrodeposition of platinum nanoflowers and their application in nonenzymatic glucose sensors, *Electrochimica Acta* **63** (2012) 1-8. https://doi.org/10.1016/j.electacta.2011.11.114

[35] H. Shu, G. Chang, J. Su, L. Cao, Q. Huang, Y. Zhang, T. Xia, Y. He, Single-step electrochemical deposition of high performance Au-graphene nanocomposites for nonenzymatic glucose sensing, *Sensors and Actuators, B: Chemical* **220** (2015) 331-339. https://doi.org/10.1016/j.snb.2015.05.094

[36] C. Shen, J. Su, X. Li, J. Luo, M. Yang, Electrochemical sensing platform based on Pd-Au bimetallic cluster for non-enzymatic detection of glucose, *Sensors and Actuators, B: Chemical* **209** (2015) 695-700. https://doi.org/10.1016/j.snb.2014.12.044

[37] J. S. Ye, Z. T. Liu, C. C. Lai, C. T. Lo, C. L. Lee, Diameter effect of electrospun carbon fiber support for the catalysis of Pt nanoparticles in glucose oxidation, *Chemical Engineering Journal* **283** (2015) 304-312. https://doi.org/10.1016/j.cej.2015.07.071

[38] P. Viswanathan, J. Park, D.K. Kang, J. D. Hong, Polydopamine-wrapped Cu/Cu(II) nano-heterostructures: An efficient electrocatalyst for non-enzymatic glucose detection, *Colloids and Surfaces A: Physicochemical and Engineering Aspects* **580** (2019) 123689. https://doi.org/10.1016/j.colsurfa.2019.123689

[39] Y. Zhang, L. Su, D. Manuzzi, H. V. E. de los Monteros, W. Jia, D. Huo, C. Hou, Y. Lei, Ultrasensitive and selective non-enzymatic glucose detection using copper nanowires, *Biosensors and Bioelectronics* **31** (2012) 426-432. https://doi.org/10.1016/j.bios.2011.11.006

[40] Y. Hu, X. Niu, H. Zhao, J. Tang, M. Lan, Enzyme-free amperometric detection of glucose on platinum-replaced porous copper frameworks, *Electrochimica Acta* **165** (2015) 383-389. https://doi.org/10.1016/j.electacta.2015.03.036

[41] L. Parashuram, S. Sreenivasa, S. Akshatha, V. Udayakumar, S. Sandeep kumar, A non-enzymatic electrochemical sensor based on ZrO_2:Cu(I) nanosphere modified carbon paste electrode for electro-catalytic oxidative detection of glucose in raw Citrus aurantium var. sinensis, *Food Chemistry* **300** (2019) 125178. https://doi.org/10.1016/j.foodchem.2019.125178

[42] M. Li, J. Yang, M. Lu, Y. Zhang, X. Bo, Facile design of ultrafine Co_7Fe_3 nanoparticles coupled with nitrogen-doped porous carbon nanosheets for non-enzymatic glucose detection, *Journal of Colloid and Interface Science* **555** (2019) 449-459. https://doi.org/10.1016/j.jcis.2019.07.099

[43] C. Guo, H. Li, X. Zhang, H. Huo, C. Xu, 3D porous CNT/MnO_2 composite electrode for high-performance enzymeless glucose detection and supercapacitor application, *Sensors and Actuators, B: Chemical* **206** (2015) 407-414. https://doi.org/10.1016/j.snb.2014.09.058